The LINNEAN SOCIETY of London BIOLOGICAL Journal of the Linnean Society

Biological Journal of the Linnean Society, 2013, **108**, 600–618. With 7 figures

Pectoral girdle and forelimb variation in extant Crocodylia: the coracoid–humerus pair as an evolutionary module

BEATRIZ CHAMERO, ÁNGELA D. BUSCALIONI* and JESÚS MARUGÁN-LOBÓN

Unidad de Paleontología, Departamento de Biología, Universidad Autónoma de Madrid, 28049 Madrid, Spain

Received 8 May 2012; revised 6 September 2012; accepted for publication 6 September 2012

To date, all statements about evolutionary morphological transformation in Crocodylia have essentially been based on qualitative observations. In the present study, we assessed the morphological variation and covariation (integration) between the scapula, coracoid, humerus, radius, and ulna of 15 species of Crocodylidae, Alligatoridae, and Gavialis + Tomistoma using three-dimensional geometric morphometrics. The results obtained reveal that the variation of elements within species (intraspecific) is large. However, despite this variability, variation across species (interspecific) is mainly concentrated in two dimensions where the disparity is constrained: 'robusticity' and 'twist' (forelimbs) and 'robusticity' and 'flexion' (pectoral girdle). Robusticity (first dimension of variation) embodies a set of correlated geometrical features such as the broadening of the girdle heads and blades, or the enlargement of proximal and distal bone ends. The twist is related to the proximal and/or distal epiphyses in the forelimb elements, and flexion of the scapula and coracoid blades comprises the second dimension of variation. In all crocodylians, forelimb integration is characterized by the strong correlations of a humerus–ulna–radius triad and by a radius–ulna pair, thus forming a tight forelimb module. Unexpectedly, we found that the humerus and coracoid form the most integrated pair, whereas the scapula is a more variable and relatively independent element. The integration pattern of the humerus–coracoid pair distinguishes a relatively robust configuration in alligatorids from that of the remainder groups. The patterns of variation and integration shared by all the analyzed species have been interpreted as an inherited factor, suggesting that developmental and functional requirements would have interacted in the acquisition of a semi-aquatic and versatile locomotion at the Crocodylia node at least 65 Mya. Our findings highlight the need to incorporate the humerus–coracoid pair in biodynamic and biomechanical studies. *Biological Journal of the Linnean Society*, 2013, **108**, 600–618.

ADDITIONAL KEYWORDS: geometric morphometrics – integration – morphological variation.

INTRODUCTION

In modern crocodiles (the crown group Crocodylia *sensu* Benton & Clark, 1988), most parts of the anatomy related to locomotion are very similar across species (Erickson *et al*., 2012). All crocodilian clades (i.e. Alligatoridae, Crocodylidae, and Gavialidae) have equivalent morphological and functional patterns (Meers, 2003; Fujiwara, Taru & Suzuki, 2010), leading to the conclusion that, comparatively, the appendicular skeleton of these animals, which includes the limbs and the girdles, is 'conservative'. Although the main difference between the crown group Crocodylia and its closest relatives is the proportional size of the fore- and hindlimbs (i.e. the robustness and length of long bones; Brochu, 1999), character-based studies within the crown reveal a high degree of fore- and hindlimb homoplasy. The key to the notion of conservativeness is the duration of such phenotypic similarity from the time of the origin of Crocodylia (65 Mya) onwards based on the occupation of analogous ecological niches by all modern crocodylians.

However, such post-cranial conservativeness is inconsistent with features in the evolution of

*Corresponding author. E-mail: angela.delgado@uam.es

Crocodylomorpha, which is characterized by a suite of forelimb autopodial and pectoral girdle novelties (Benton & Clark, 1988; Müller & Alberch, 1990; Buscalioni *et al*., 1997). Drastic morphological changes took place at the base of its crown group (Crocodylia), modifying the skeletal postures, which had consequences for the exploitation of new and more versatile locomotor behaviours (Frey, 1982, 1988; Salisbury & Frey, 2001; Salisbury *et al*., 2006). Thus, the available evidence suggests that the skeletal transformation of the crocodylian locomotor apparatus entailed a novel anatomical relationship between the pectoral girdle and the appendicular skeleton, although the integration of these elements has never been studied. Interestingly, the fact that bipedality is prominent throughout Archosauria (Gatesy, 1991; Gatesy & Middleton, 1997; Reilly & Elias, 1998; Farlow *et al*., 2005; Reilly *et al*., 2005) may have contributed to the morphological importance of the forelimb and the pectoral girdle in crocodile evolution being overlooked. Until now, statements about morphological similarity in crocodiles have essentially been based on qualitative observations (Mook, 1921; Romer, 1924), some of which have been evaluated phylogenetically (Brochu, 1997a). Given that post-cranial shape differences may be subtle, in the present study, we propose a formal morphometric approach for understanding the degree of skeletal similarity among crocodylians.

Relying on the knowledge that tetrapods maintain a standard pattern of modular limb organization regulated by *HoxD* genes (Shubin, Tabin & Carroll, 1997; Young & Hallgrímsson, 2005; Young, 2006), most studies have analyzed patterns of integration between homologous fore- and hindlimb elements (for a compendium of cases, see Villmoare, Fish & Jungers, 2011). However, only a few have attempted to understand girdle and limb shape integration (Gatesy & Middleton, 1997; Rasskin-Gutman & Buscalioni, 2001; Young & Hallgrímsson, 2005; Young, 2006), despite their close evolutionary and functional association. In the present study, we investigate the elements of the pectoral girdle and forelimb (scapula, coracoid, humerus, radius and ulna) using three-dimensional (3D) geometric morphometrics in 15 crocodylian species. In particular, these tools allow the degree of morphological variation and integration of the skeleton (Olson & Miller, 1958) to be scrutinized at an unprecedentedly high level of resolution (Klingenberg, 2009). We explore the correlation between 3D-shape characters, their relationship with size, and the covariation among elements, to address: (1) the intraspecific shape variation of each element; (2) the dimensionality and limits of interspecific morphological variation (i.e. disparity) among members of the crown Crocodylia; and (3) the covariation of limb and girdle elements and their morphological trends within a phylogenetic context. Finally, we reconstruct the evolution of the anterior appendage within Crocodylia, examining how girdle and limb shape integration has mediated the acquisition of a modern semi-aquatic locomotion habit.

MATERIAL AND METHODS

Sample

The studied sample encompasses eight genera and 15 species of adult and subadult specimens of Crocodylia (*Alligator mississippiensis* Daudin 1802; *A. sinensis* Fauvel 1879; *Caiman crocodilus* Linnaeus 1758; *Caiman yacare* Daudin 1802; *Melanosuchus niger* Spix 1825; *Paleosuchus palpebrosus* Cuvier 1807; *Paleosuchus trigonatus* Schneider 1801; *Crocodylus acutus* Cuvier 1807; *Crocodylus moreletii* Duméril & Bibron 1851; *Crocodylus niloticus* Laurenti 1768; *Crocodylus rhombifer* Cuvier 1807; *Crocodylus siamensis* Schneider 1801; *Osteolaemus tetraspis* Cope 1861; *Tomistoma schlegelii* Müller 1838; *Gavialis gangeticus* Gmelin 1789) from the Florida Natural History Museum (Gainesville, FL, USA). The sample spans a wide range of crocodylian diversity (63% of all species) and disparity. Phylogenetic relationships between species follow the hypothesis of Gatesy *et al*. (2003) in which *T. schlegelii* is the sister taxon of *G. gangeticus* (Fig. 1). Five elements comprising the appendicular and pectoral skeleton (i.e. scapula, coracoid, humerus, ulna, and radius) were analyzed. Post-cranial elements are still lacking in collections and, in accordance with the completeness of specimens in the collection, the sample size for each element varies (see Supporting information, Appendix 1, which also includes measurements of femoral length; note that, in one *C. niloticus* and one *T. schlegelii*, there is a difference in size as a result of immaturity). The Supporting information (Appendix 2) also provides measurements of the humeral and coracoid lengths of extinct Crocodyliformes and extant species. These data have been used to discuss the anterior appendage evolution.

Anatomy of the anterior appendage

The osteology of the crocodylians forelimb and pectoral girdle was previously described by Mook (1921). More recently, the position, orientation, and muscular anatomy of the anterior appendicular elements has been described in detail by Meers (2003) and Schwarz, Frey & Martin (2006). The scapulocoracoid complex forms the pectoral girdle and they articulate in a synchondrosis suture that becomes fused along ontogeny (Brochu, 1995). The shoulder joint is hemisellar and posteroventrally directed (Jenkins, 1993). The scapula and the coracoid are

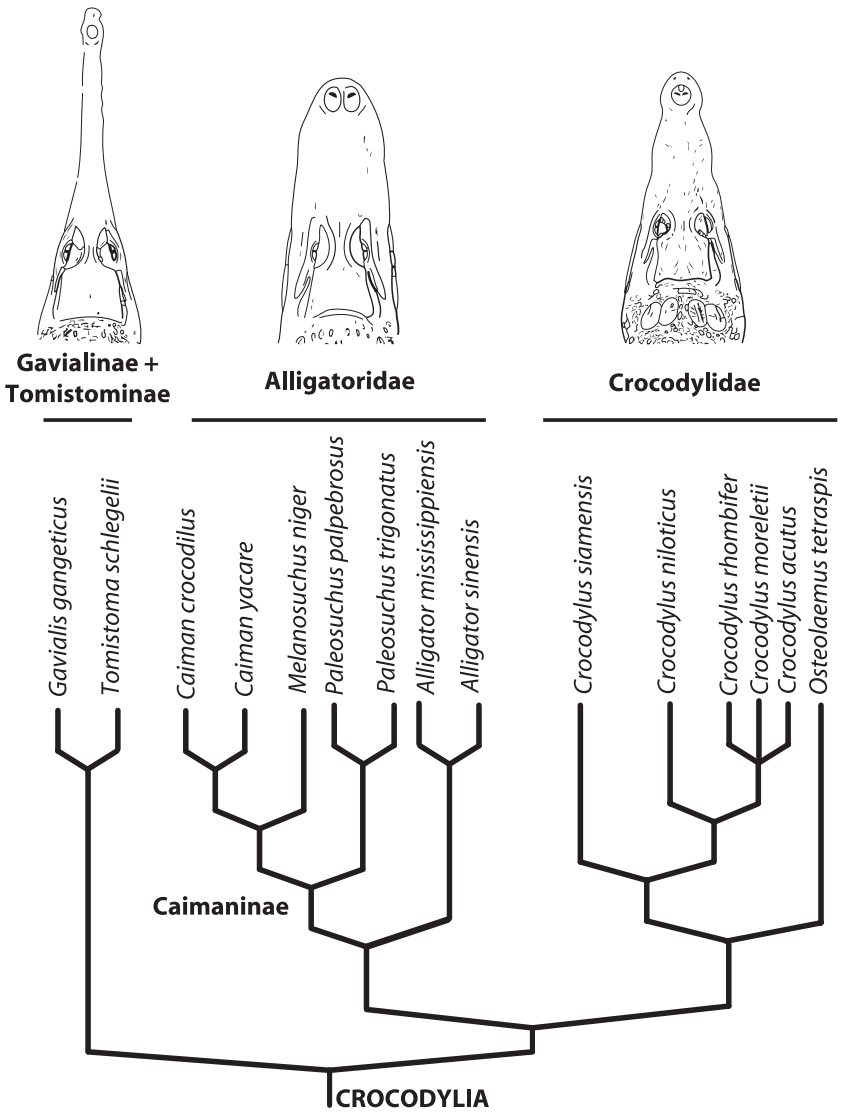

Figure 1. Cladogram of the crown Crocodylia *sensu* Gatesy *et al*. (2003) in which the non-analyzed taxa have been pruned. According to this phylogenetic hypothesis, Crocodylia is defined as the last common ancestor of *Gavialis* + *Alligator* + *Crocodylus*, and all of its descendant. *Tomistoma* and *Gavialis* are sister taxa and placed in an unnamed node, representing the long-snouted crocodylians. Alligatoridae, with wide and short skulls, gathers the two species of *Alligator* plus the caimans (Caimaninae). The genera *Crocodylus* + *Osteolaemus*, with a high variability of skull length and width, conform the node Crocodylidae. Skull figures are modified from Wermuth & Fuchs (1978).

approximately the same length as that in Crocodylia. The scapular blade is caudally inclined approximately 50° to the horizontal plane, whereas the long axis of the coracoidal blade is curved. The distal part of the coracoid is ventromedially directed and forms a mobile joint with the cartilagous sternum. The cartilagous sternal elements, together with the ventromedial coracoidal edge, form the floor of the thoracic cavity. The anatomy of the forelimb elements is characterized by the presence of articular cartilages that provide complex 3D joint surfaces *in vivo* (Fujiwara *et al*., 2010). The post-mortem decomposition of cartilages leaves articular bone surfaces with less relief. The humeral shape changes significantly when chondroepiphyses are removed (Bonnan *et al*., 2010). Nevertheless, conspicuous articular bone eminences (in the humeral head) and depressions (in the distal condyles), as well as tuberosities (ulnar olecranon process) and crests (humeral dectopectoral), are distinctly marked in the forelimb osteology. The performance of the anterior appendicular skeleton is directly related to the braking impulse of forelimbs in terrestrial and aquatic locomotion (Willey *et al*., 2004), and

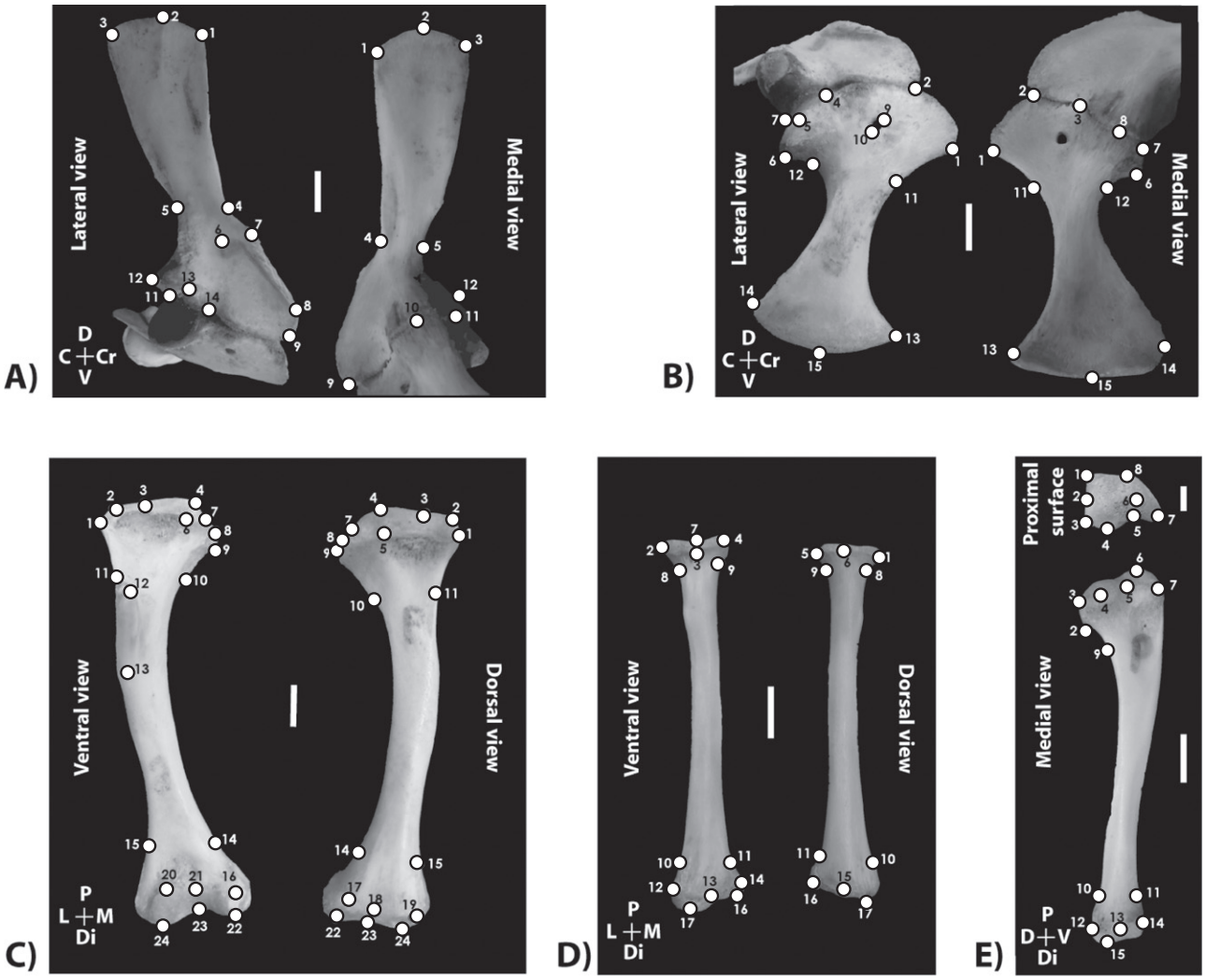

Figure 2. Landmark configurations of the pectoral girdle and forelimb bones exemplified over *Caiman* (right elements). A, scapula; B, coracoid; C, humerus; D, radius; E, ulna. In each image, a diagram of bone orientations is depicted at the lower-left corner. C, caudal; Cr, cranial; D, dorsal; Di, distal; M, medial; L, lateral; P, proximal; V, ventral; Scale bar: 1 cm (for landmark definitions, see Table 1).

indirectly with respiration through the costosternal movement (Claessens, 2009).

Landmarks

For each isolated bone, a configuration of landmarks was digitized in 3D with a Microscribe G2 (Immersion Co.) (Fig. 2, Table 1). The landmarks capture the most salient features of the bones and have been designed to reflect the geometry of their distal and proximal articular surfaces, the orientation of epiphyses with respect to each other, and the disposition of the pectoral blades with respect to their articular areas. None of the landmarks reflect muscular insertions and origins. The homology of midshaft landmarks is too ambiguous, and so these landmarks have not been used. Mostly, elements from the right side were analyzed, although, when this was unavailable, the left side was selected and then mirrored. Obviously, to analyze covariation, only bones from the same individual and side were considered. The nomenclature of bone orientation matches that of Meers (2003). The advantage of working in 3D is that the methodology can capture spatial properties never previously analyzed for the studied elements (such as flexing, stretching, and twisting of each element), providing information about the relative position of salient features and the relative proportions of their parts. However, using landmark data, we had to ignore the planar blades and thicknesses of the crests (e.g. deltopectoral, acromial).

Table 1. Landmark descriptions

Landmark	Description
Scapula	
1	Cranial border of the dorsal edge of the scapular blade: craniodorsal projection of the scapula
2	Maximum curvature of the dorsal edge of the scapular blade
3	Caudal border of the dorsal edge of the scapular blade: caudodorsal projection of the scapula
4	Cranial constriction of the scapular blade dorsal to the scapular head
5	Caudal constriction of the scapular blade, between the medial scapulosternal ligament and the posterior scapular tubercle
6	Mid-depression at the intersection between acromial crest and the posterior scapular tubercle
7	Maximum height of the acromial crest at the cranial edge of the scapula: scapular prominence
8	Ventral tip of the acromial crest at the cranial edge of the scapula
9	Cranioventral border of the scapular head
10	Dorsal maximum expansion of the scapulocoracoid syncondrosis in medial view at the glenoid process
11	Caudoventral point of the glenoid process in medial view
12	Caudodorsal edge of the glenoid process: scapular buttress
13	Craniodorsal edge of the glenoid process: scapular buttress
14	Caudal point of the scapulocoracoid syncondrosis in lateral view cranial to the glenoid process
Coracoid	
1	Cranial edge of the coracoid head
2	Cranial point of the scapulocoracoid syncondrosis
3	Cranial point of the expanded glenoid process at the middle of the scapulocoracoid syncondrosis in medial view
4	Cranial point of the expanded glenoid process at the posterior scapulocoracoid syncondrosis in lateral view
5	Maximum curvature of glenoid lip in lateral view
6	Caudoventral rim of the glenoid lip
7	Caudal point of the glenoid process in medial view
8	Dorsal maximum expansion of the scapulocoracoid syncondrosis in medial view at the glenoid process
9	Dorsal edge of the coracoid foramen in lateral view
10	Ventral edge of the coracoid foramen in lateral view
11	Cranial constriction of the coracoid head
12	Caudal constriction of the coracoid head
13	Cranial edge of the coracoid ventromedial blade
14	Caudal edge of the coracoid ventromedial blade
15	Maximum curvature of the coracoid ventromedial blade
Humerus	
1	Lateral edge of the lateral humeral process
2	Dorsal elevation of the lateral humeral process
3	Dorsal depression between the lateral humeral process and glenohumeral condyle
4	Dorsal elevation of the glenohumeral condyle
5	Rim of the ventral contour of the glenohumeral condyle in dorsal view (outline of the articular cartilage)
6	Rim of the ventral contour of the glenohumeral condyle in ventral view (outline of the articular cartilage)
7	Dorsal depression between the glenohumeral condyle and the medial humeral process
8	Dorsal elevation of the medial humeral process
9	Medial edge of the medial humeral process
10	Medial constriction of the humeral head at the end of the medial triceps ridge
11	Contact between the dectopectoral crest and the lateral humeral border
12	Tip of the dectopectoral crest
13	Contact between the dectopectoral crest and the lateral humeral border: dectopectoral tubercle
14	Medial constriction between the diaphysis and the distal epiphysis
15	Lateral constriction between the diaphysis and the distal epiphysis
16	Mediodorsal rim of the dorsal contour of the distal epiphysis (outline of the articular cartilage)
17	Mediodorsal rim of dorsal contour the distal epiphysis (outline of the articular cartilage)

Table 1. *Continued*

Landmark	Description
18	Intercondylar notch in dorsal aspect (outline of the articular cartilage)
19	Latero-dorsal edge of the distal epiphysis (outline of the articular cartilage)
20	Laterodorsal rim of the ventral contour of distal epiphysis (outline of articular cartilage)
21	Intercondylar notch of distal epiphysis: dorsal rim of olecranon fossa (outline of articular cartilage)
22	Caudal rim of the medial condyle of the distal epiphysis: ulnar condyle
23	Intercondylar notch of the distal epiphysis: caudal rim of olecranon fossa
24	Caudal rim of the lateral condyle of the distal epiphysis: radial condyle
Radius	
1	Dorsomedial edge of the proximal radial head: radiohumeral articular surface
2	Ventromedial edge of the proximal radial head: radiohumeral articular surface
3	Notch of the proximal radial head in ventral view at the ulnar facet
4	Ventrolateral edge process of the of the proximal radial head: radiohumeral articular surface
5	Dorsolateral edge of the proximal radial head: radiohumeral articular surface
6	Maximum curvature of the dorsal margin of the proximal radial head
7	Mid-point of the radiohumeral articular surface
8	Medial constriction of the radial head
9	Lateral constriction of the radial head
10	Medial line at the distal shaft constriction
11	Lateral line at the distal shaft constriction
12	Dorsomedial process of the radial condyle
13	Intercondylar point in ventral view (outline of the articular cartilage) dorsal to the distal radial groove
14	Laterodorsal rim of the lateral condyle
15	Maximum curvature of the dorsal margin of the distal epiphysis (outline of articular cartilage)
16	Maximum distal curvature of the lateral condyle
17	Maximum distal curvature of the medial condyle: radial articular surface
Ulna	
1	Laterodorsal edge of the proximal epiphysis: radial facet
2	Mid-point of minimal curvature of the radial facet
3	Mediodorsal edge of the proximal epiphysis: radial facet
4	Medial expansion of the ulnar-humeral surface
5	Medial notch dorsal (cranial) to the olecranon process
6	Maximum elevation of the olecranon process
7	Ventral (caudal) tip of the olecranon process
8	Lateral edge of the olecranon process
9	Dorsal (cranial) constriction of the ulnar head
10	Dorsal line at the craniolateral process, confluent with the shaft constriction at the distal epiphysis
11	Ventral (caudal) constriction of the ulnar shaft and distal epiphysis
12	Dorsal (cranial) edge of the anterior oblique process
13	Intercondylar depression in medial view of the distal epiphysis
14	Ventral (caudal) edge of the posterior oblique process
15	Distal edge of the anterior oblique process

Anatomical terms are based on Fujiwara *et al*. (2010), and Sertich & Groenke (2010), bone orientations follows Meers (2003).

Geometric morphometrics (GM) and statistical procedures were performed with MORPHOJ, version 1.02c (Klingenberg, 2011). First, the 3D landmark coordinates were superimposed using a full Procrustes fit to remove the effects of translation, rotation, and scaling (Rohlf & Slice, 1990; Bookstein, 1991). Implementing the Procrustes fit in MORPHOJ includes a reflection of the data so that the differences between left and right elements are removed (Dryden & Mardia, 1998). Principal component analyses (PCA) were used to summarize the variance of shape data (the resulting x and y coordinates after the Procrustes superimposition) of each element across the sample. This methodology decomposes the variance in

orthogonal dimensions as linear combinations of the original data (principal components; PCs). To corroborate the phylogenetic structure of the data, we performed a phylogenetic contrast on the Procustes data using MORPHOJ (Klingenberg & Gidaszewski, 2010). In addition, to trace the evolutionary history of geometric variation, the cladogram (Fig. 1) was implemented in the PCA ordinations, reconstructing the internal nodes using the unweighted square parsimony method (Maddison, 1991; Rohlf, 2002). The two-block partial least squares method (2B-PLS; Rohlf & Corti, 2000) was used to assess the patterns of pairwise covariation of the Procustes data between elements.

Although PCA is an essential tool in GM for analyzing shape variance, the 2B-PLS is less widely used and thus warrants a brief explanation. The method is similar to PCA in that it generates new variables that are combinations of the original ones, although it differs in that its dimensions are interblock generated, and its components are ordered by their covariance instead of their explained variance. Thus, the new variables computed by the method are ordered in accordance with the explained (and maximum) covariance between the two blocks of original variables (Marugán-Lobón & Buscalioni, 2006). To test the null hypothesis of complete independence (i.e. that the observed covariation is random) between the two blocks of variables, permutation tests were performed. In addition, the R_V coefficient (Klingenberg, 2009) was calculated as an overall measure of the association between the two blocks (values in the range 0–1, where 1 denotes complete correlation). The results are shown on warped computed tomography-scanned templates of each bone, using LANDMARK EDITOR (Wiley, 2006).

RESULTS

Morphological variation of single elements

In all of the studied elements, the first dimension of the PCA (PC1) accounts for a gradient of differential robusticity, whereas the variation represented by PC2 is associated with the relative orientation of bone parts. Explained variance for each element is expressed in its corresponding graph (Figs 3, 4). The term 'robusticity' encompasses a set of geometrical features such as the broadening of the girdle heads and blades, and the enlargement of the proximal and distal bone ends. The shaft diameter of limb bones encompasses the relative epiphyseal enlargement. Different orientations in the pectoral girdle are related to the angular relationship between their planar surfaces (scapular and coracoid blades) and their articulation heads. The term 'flexed' is used when the coracoscapular disposition is denoted by a more or less acute angular relationship and the blade is bowed. In each of the forelimb elements the observed variation is correlated with changes in the relative orientations of the distal and proximal epiphyses. We express this geometry as 'twisted'.

Pectoral girdle

Scapula

In the ordination, the caimans (*Caiman*, *M. niger*, and one specimen of *P. palpebrosus*) and the crocodylid species (*C. siamensis* and *Crocodylus porosus-siamensis*) all have positive scores for PC1. This distribution is associated with the scapular blade, which tends to be narrower and with almost parallel edges (Fig. 3A, B). This finding is consistent with the synapomorphy in caimans addressed by Brochu (1997b). The negative extreme is occupied by *Gavialis*, *Alligator*, and some species of *Crocodylus* with more robust scapulae, whereby the scapular blade is broader and its dorsal margin flares. Moreover, in the latter taxa, the cranial edge of the scapular blade is straight, whereas the caudal edge is strongly concave. *Gavialis* is also placed in a congruent position, bearing the plesiomorphic condition of a more dorsally flared scapula, as suggested by Brochu (1997b). However, the position of *Alligator* is incongruent with qualitative characters (Brochu, 1997b). In light of this distribution, the scapula does not allow a clear-cut segregation of families (Fig. 3A).

It should also be noted that, besides the aforementioned gradients, PC1 encompasses correlated shape changes between the scapular blade edges and the axis of the scapulocoracoid (Fig. 3B). In *Gavialis* (negative values), the scapular blade is cranially concave, and caudally rectilinear, whereas the orientation of the scapulocoracoid axis is less oblique relative to the longitudinal axis of the scapula. However, in *Caiman*, whose dorsal scapular margin is narrower, the cranial and caudal blade edges are almost parallel to each other, and the scapulocoracoid axis orientation is strongly oblique relative to the scapular longitudinal axis.

Coracoid

PC1 shows a gradation of craniocaudal width matching a segregating ordination between the crocodylian families (Fig. 3C, D). For the positive PC1 values, alligatorids show both ventrally and dorsally expanded edges (i.e. the coracoid ventral edge is flared and the proximal head is craniocaudally wider). The articulation surface is also wider and almost perpendicular to the main axis of the coracoid. With more negative values, *Gavialis*, *Tomistoma*, and crocodylids have narrower coracoid dorsal and ventral

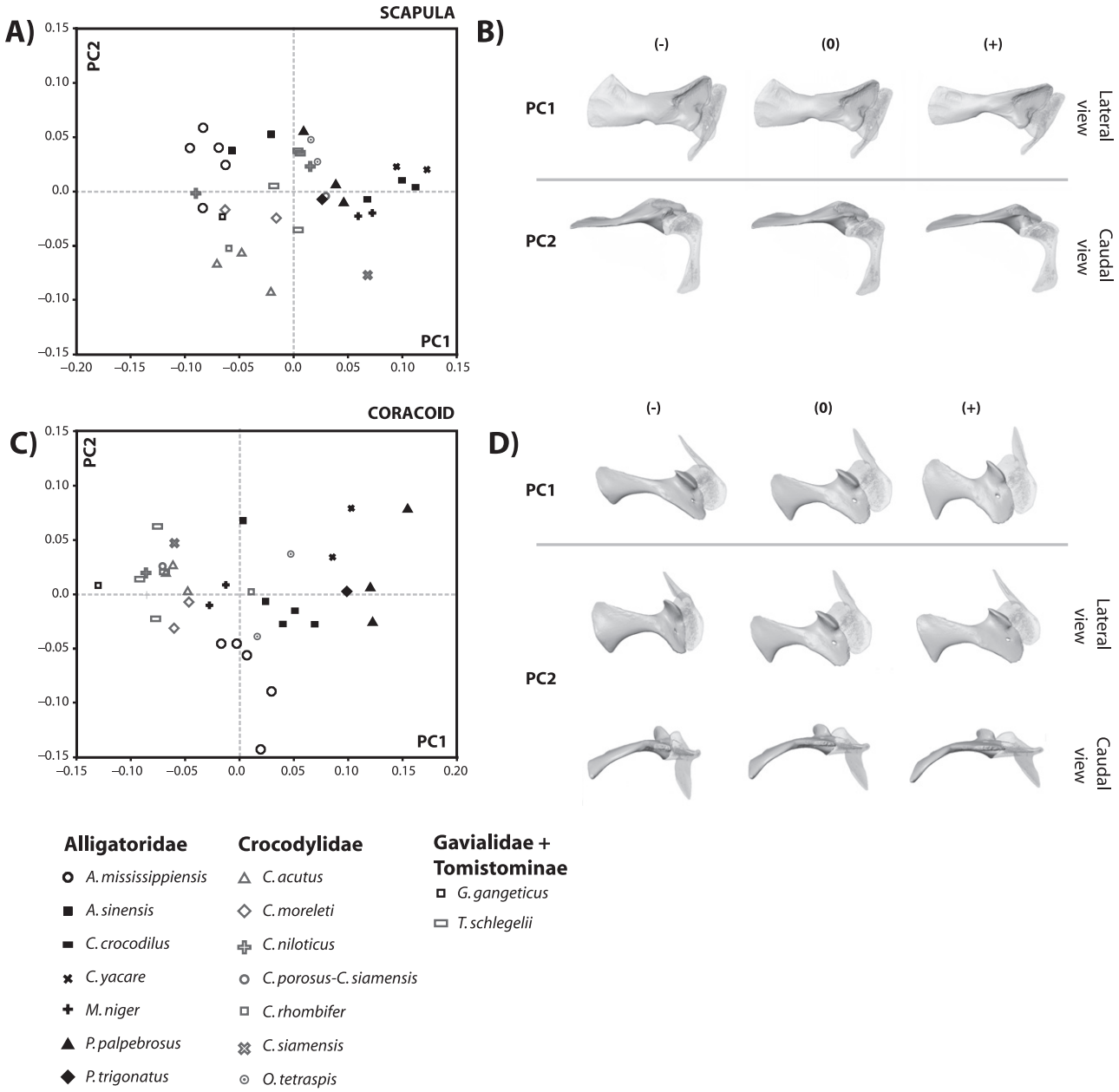

Figure 3. Principal component analysis (PCA) of the pectoral girdle elements. A, scatter plot of PC1 (*x*-axis; 31.95% variance explained) versus PC2 (*y*-axis; 13.21% variance explained) of the scapula. B, computed tomography (CT)-scan morphing of the scapula to show variation encompassed by PC1 and PC2. C, scatter plot of PC1 (*x*-axis; 28.33% variance explained) versus PC2 (*y*-axis; 13.53% variance explained) of the coracoid. D, CT-scan morphing of the coracoid to show variation encompassed by PC1 and PC2.

extensions with an almost constant bone width. The articulation surface forms an angle with the main axis of the coracoid. In addition to flexion, PC2 variability is associated with the relative proportions and the shape of the articular head and the shaft.

No discrete characters in the coracoids have been used to distinguish crocodylian families in previous phylogenetic analyses. Only the thickness of the scapulocoracoid facet, anterior to the glenoid fossa (Brochu, 1997b) segregates alligatorids and crocodylids (with *Crocodylus cataphractus* being an exception) from gavialoids. However, this particular character cannot be captured with our landmark configuration.

Forelimb

Humerus

The ordination of taxa for humeral variation is similar to that of the coracoids, thus segregating Alligatoridae from the rest. However, here, the combination of PC1 and PC2 contributes to the taxonomic separation between families (Fig. 4A). Alligatoridae have distal and proximal epiphyses that are lateromedially wider (robust humeri in PC1) and less twisted (according PC2) than they are in Crocodylidae and *Tomistoma* + *Gavialis*. Note that the analysis detects a correlation between humeral robusticity and the arrangement of the deltopectoral crest. In accordance with the character qualitatively defined by Brochu (1997b; see also, Salisbury *et al*., 2006), the deltopectoral crest emerges more gradual from the proximal end of the humerus or abruptly. Both character states are represented in the results of the present study. The abrupt emergence of the dectopectoral crest is associated with robust humeri, whereas, in slender humeri, the deltopectoral crest is smoother. The general geometry of the humerus of the three crocodylian families indicates that *Gavialis* is grouped within crocodylids because it shows the same pattern of shape variation. Furthermore, the twist and the dorsoventral thickness of the bone (PC2) involve the orientation of proximal and distal epiphyses relative to each other, such that, if the humerus is twisted, the proximal epiphysis is turned mediodorsally, whereas the distal articular axis is turned medioventrally (Fig. 4B).

Radius

The general pattern of bone robusticity observed in the radius (PC1) is correlated with the orientation of the proximal epiphysis (Fig. 4C, D). In the ventral view, the proximal epiphysis bends either medially (positive value) or laterally relative to the main axis of the radius. PC2 accounts for the twist of the radii, in which both epiphyses face opposite sides (i.e. the proximal and distal ends respectively twist laterov-entrally and laterodorsally).

The ordination does not segregate families as in the previous bones, even if the analysis is repeated with data from the two outliers (*C. acutus* UF98068 and *C. moreletii* UF5481; data not shown) excluded.

Ulna

The robusticity of the ulna (PC1) is correlated with the angle of the articular axis of the proximal epiphysis relative to the shaft (Fig. 4E, F). PC2 accounts for the relative twist of the ulnae, with changes only on the distal epiphysis (ventromedially turned). The shaft constriction at the proximal end is more marked for more positive values, with the orientation of the articular proximal surface being more oblique relative to the axis bone. As the radius, the ulna does not show a clear-cut taxonomic segregation of families.

Integration patterns

Table 2 shows the statistical significance and degree of association (R_V coefficient) between pairs of

Table 2. Results of the two-block partial least squares analyses between pairs of elements

	Scapula	Coracoid	Humerus	Radius	Ulna
Scapula	–	**< 0.0001**	0.004	**< 0.0001**	**0.0001**
Coracoid	**0.4360**	–	**< 0.0001**	0.008	**< 0.0001**
Humerus	0.3459	***0.6023***	–	**< 0.0001**	**< 0.0001**
Radius	**0.3769**	0.3376	**0.5118**	–	**< 0.0001**
Ulna	**0.4423**	**0.4661**	***0.6056***	***0.6707***	–

Grey boxes show the *P*-values from the permutation tests. The null hypothesis of complete independence between the two blocks is rejected ($P < 0.001$; 1000 permutations). Pairs of elements with a statistically significant association are shown in bold. White boxes show the R_v coefficients of the overall degree of association. Those with significant associations ($P < 0.001$) are shown in bold, whereas those with the highest covariation are shown in italics.

Figure 4. Principal component analysis (PCA) of forelimb elements. A, scatter plot of PC1 (*x*-axis; 26.29% variance explained) versus PC2 (*y*-axis; 16.23% variance explained) of the humerus. B, computed tomography (CT)-scan morphing of the humerus to show variation encompassed by PC1 and PC2. C, scatter plot of PC1 (*x*-axis; 34.49% variance explained) versus PC2 (*y*-axis; 15.12% variance explained) of the radius. D, CT-scan morphing of the radius to show variation encompassed by PC1 and PC2 in the radius. E, scatter plot of PC1 (*x*-axis; 27.08% variance explained) versus PC2 (*y*-axis; 12.53% variance explained) of the ulna. F, CT-scan morphing of the ulna to show variation encompassed by PC1 and PC2.

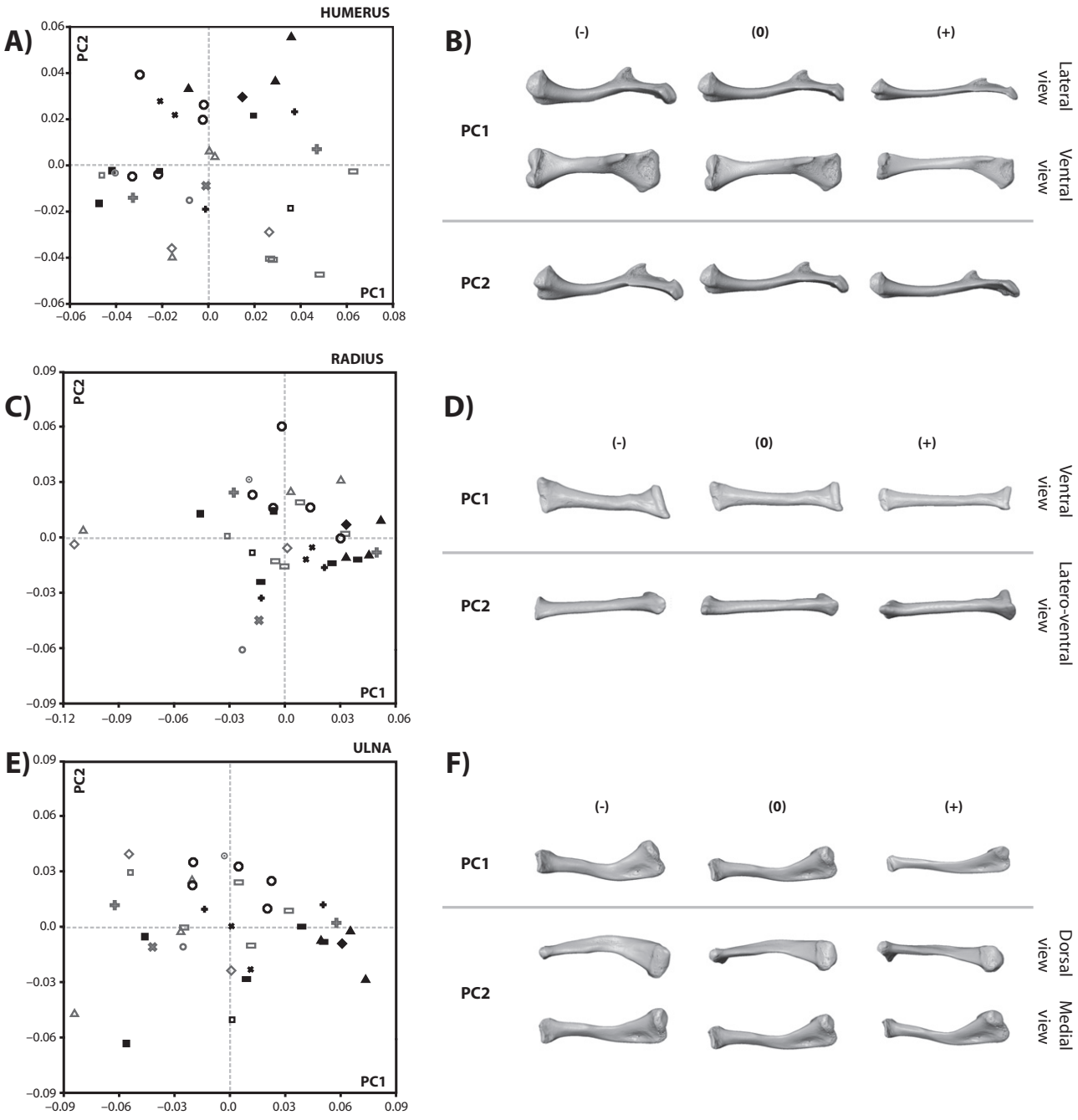

Alligatoridae

- *A. mississippiensis*
- *A. sinensis*
- *C. crocodilus*
- *C. yacare*
- *M. niger*
- *P. palpebrosus*
- *P. trigonatus*

Crocodylidae

- *C. acutus*
- *C. moreleti*
- *C. niloticus*
- *C. porosus-C. siamensis*
- *C. rhombifer*
- *C. siamensis*
- *O. tetraspis*

Gavialidae + Tomistominae

- *G. gangeticus*
- *T. schlegelii*

Table 3. Results of the multivariate linear regression analysis of shape on size

	Scapula	Coracoid	Humerus	Radius	Ulna
Percentage shape prediction	9.8454	9.2395	7.6953	7.2535	14.2243
P	< 0.001	0.003	0.008	0.031	< 0.001

The null hypothesis of complete independence between the two blocks is rejected ($P < 0.001$; 1000 permutations). Notice that size only explains statistically significant variation on shape in the scapula and the ulna.

elements. The results indicate that all pairwise comparisons are statistically significant, with the exception of the scapula–humerus and coracoid–radius pairs. The scatter plot of pairs with highest covariances illustrates a common trend for all analyzed species (Fig. 5A, C, E). Most of the statistically significant pairs are associated by relative robusticity (Fig. 5B, D). However, among the highest associations, only the coracoid–humerus pair has a taxonomic signal, with which alligatorids may be segregated from the remainder. This dimension of correlation relates to two different organizations: (1) relatively narrow coracoids (Fig. 5A, B) with relatively slender humeri (and a smooth medially facing dectopectoral crest) and (2) dorsally and ventrally expanded coracoids with relatively broad humeri (with an abrupt and laterally oriented dectopectoral crest). Alligatorids tend to have stouter humeri and coracoids than the remainder crocodylians. *Osteolaemus tetraspis* and *C. rhombifer* are incorrectly categorized because they are located within the alligatorids, whereas *M. niger* is grouped within Crocodylidae. Indeed, the former two crocodylids (*O. tetraspis* and *C. rhombifer*) species are recurrently associated with alligatorids in other morphometric studies because they feature convergences in their skulls (Sadleir & Makovicky, 2008; Piras *et al*., 2009). The grouping of *Melanosuchus* is an unexpected convergence.

It is worth noting that the robust configuration in alligatorids notably differs from the longirostral species *T. schlegelii* and *G. gangeticus* (Fig. 5A). Consistent with this, Meers (2003) found that the extension and disposition of the coracoid musculature in *Gavialis* (with the narrowest coracoid) is associated with its aquatic and singular locomotor habits.

DISCUSSION

The present study aimed to assess different organismic levels of phenotypic similarity within crown Crocodylia. The analyses revealed that the variation of elements within species (intraspecific) is large and equivalent across species (interspecific). We also found that the integration (covariation) of elements among taxa is the same; thus, all crocodylians share an almost identical pattern of integration. However, we unexpectedly found connected pairs of elements (coracoid–humerus) that show a phylogenetic significance.

The first level of similarity that we found (i.e. the variation of single elements) implies that, within Crocodylia, the shape of each element changes significantly across the sample, such that even individuals of the same species do not cluster together. The great variability of the humerus in *A. mississippiensis* has previously been stressed in comparison with Aves (*Numida meleagris* and *Struthio camelus*; Bonnan *et al*., 2010). Such variability could be related to reaction norms and the unique histological conditions in Crocodylia, such as the effect of incubation temperature on growth and development (Deeming & Ferguson, 1989), and to characteristic bone–tendon and bone–ligament interfaces that may shape bone growth (Suzuki, Murakami & Minoura, 2003). The latter study stressed that the fibrocartilage can differentiate into bone *in vivo* at the epiphyseal areas in long bones. Furthermore, these intraspecific differences are also ubiquitous in forelimb musculature (*A. mississippiensis*), which has been interpreted as random variation or unknown selection pressures on the forelimb anatomy (Meers, 2003). This variability (and possibly its causes) may not be unique to *A. mississippiensis*, and may be a common feature of the crown-group Crocodylia.

A second level of analysis reveals that the variation of each element is mainly constrained in two dimensions: robusticity and twist (in the forelimbs) and robusticity and flexion (in the pectoral girdle). In all the analyses of isolated bones, the variation is analogously related to relative robusticity (PC1, first dimension of variation), the relative increase in volume of distal and proximal articulations in forelimb elements, and the craniocaudal expansion for pectoral elements. The twist is related to the proximal and/or distal epiphyses in forelimb elements, and the flexion for scapula and coracoid blades (PC2, second dimension of variation).

In principle, geometric differences interpretable as robusticity (i.e. the broadening of girdle heads and blades, or the enlargement of proximal and distal bone ends) could be associated with allometry if they

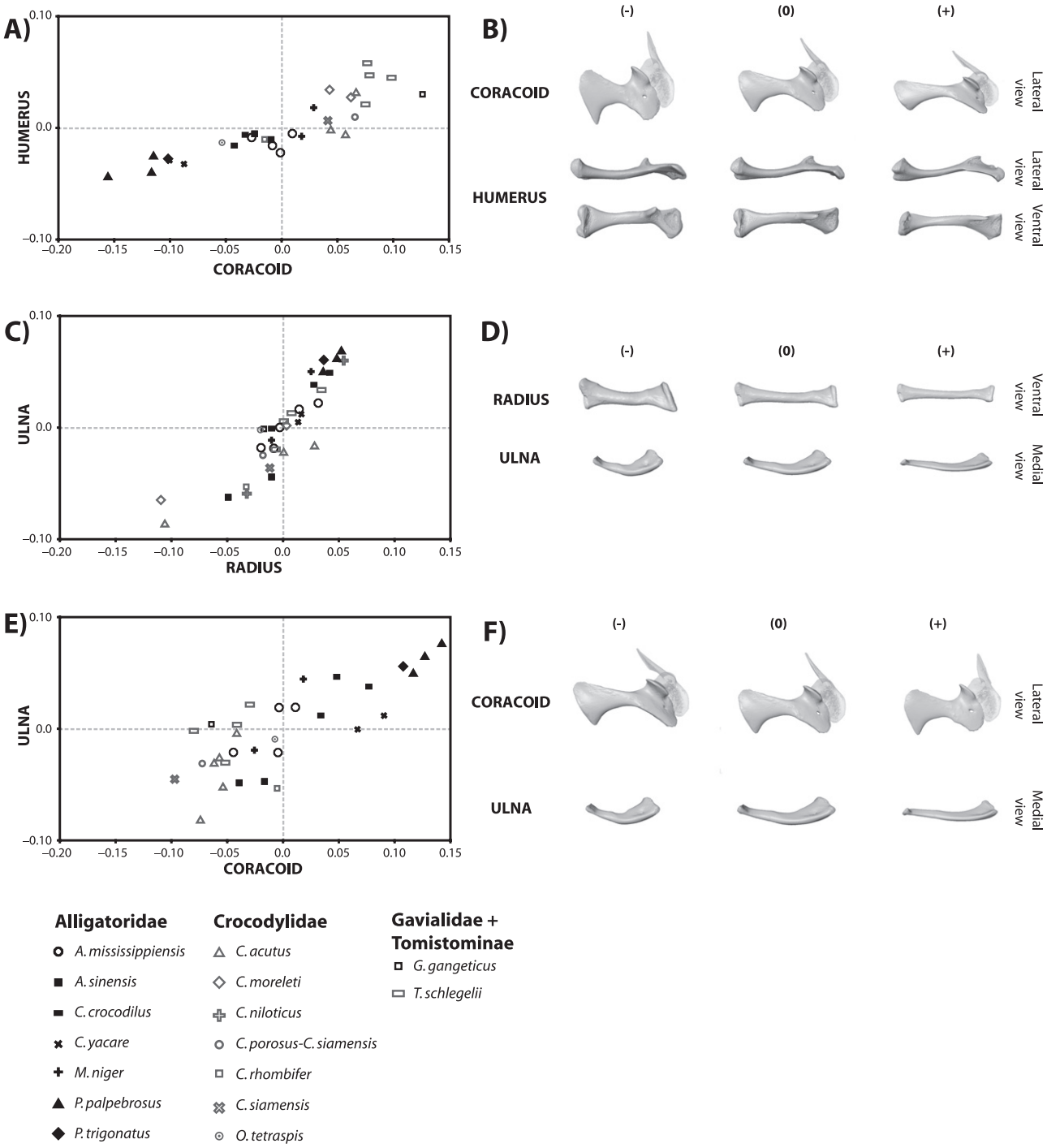

Figure 5. Results of the two-block partial least squares (2B-PLS) analysis. A, B, scatter plot of the resulting covariation between the humerus–coracoid pair, and computed tomography (CT)-scan morphing of the bones to show shape changes encompassed by the covariation. C, D, scatter plot of the resulting covariation between the ulna–radius pair, and CT-scan morphing of the bones to show shape changes encompassed by the covariation. E, F, scatter plot of the resulting covariation between the ulna–coracoid pair, and CT-scan morphing of the bones to show shape changes encompassed by the covariation. For the correlations between pairs of elements, see Table 2.

were correlated with size. However, multivariate regressions revealed no statistical support for a significant influence of size upon shape, except for the scapula and ulna (Table 3). We found that, as the size increases, the scapular constriction widens, and the cranial margin becomes convex, whereas the caudal margin becomes more concave. The proximal ulnar epiphysis enlarges, changing the shape of the olecranon process. Analogous results for the increase of the olecranon process relative to ulna size were obtained by Livingston *et al*. (2009) in their study of limb scaling in *A. mississippiensis*. The fact that size does not influence robusticity implies that small to medium body-sized alligatorids, such as *Caiman* and *Paleosuchus*, have highly robust humeri and coracoids.

Therefore, our morphometric analyses substantiate the view that, within modern members of the crown group Crocodylia, the shape of the anterior appendicular skeleton has a high degree of homoplasy, although the variation of appendicular bone 3D shape characters is dimensionally limited (i.e. disparity is constrained). Namely, for the ulna, the radius, and the scapula, species are mixed in a delimited gradient throughout morphospace. By contrast, for the coracoid and humerus, there is a taxonomic segregation such that members of Alligatoridae, Crocodylidae, and the longirostrine *Tomistoma* + *Gavialis* cluster together. Arguably, the phenotypic similarity of these bones is explained by the phylogenetic relatedness among the terminal taxa at each clade. In particular, this is clear for the coracoid (coracoid $P = 0.0006$ over 10 000 permutations; Fig. 6). Moreover, the resulting patterns of trait covariation (i.e. integration) with the 2B-PLS analyses provide a way of interpreting this result.

In crocodylians, forelimb integration is characterized by the strong correlations of a humerus–ulna–radius triad and by a radius–ulna pair, thereby forming a tightly integrated forelimb module (Table 2). This highly constrained correlation pattern is visible in Figure 5C. In principle, the integration should be greatest between adjacent bones belonging to equivalent developmental fields (Riska, 1986; Klingenberg, 2008), and between elements sharing adjacent articular joints (i.e. scapula and coracoid) and limb elements (Chernoff & Magwene, 1999). Integration of this form in a seriated structure such as the limb has been reported for birds (Magwene, 2001) and mammals (Young & Hallgrímsson, 2005). Unexpectedly, however, we found that the humerus and the coracoid (but not the scapula–coracoid pair) is the most highly integrated pair. Thus, in Crocodylia, the phenotypic variation in the coracoid is closely associated with the humerus, whereas the scapula appears to be the more variably and relatively independent element. It is noteworthy that this result is congruent with the singular developmental program of the tetrapod scapula, in which the blade is derived from several adjacent but independent portions whose variance may be closely related to epigenetic factors associated with muscle attachments (Matsuoka, Ahlberg & Kessaris, 2005; Young, 2006).

The alligatorid divergence

The relevance of the humerus–coracoid pair is perceived in Alligatoridea divergence from the remainder clades, tending to have stouter humeri and coracoids. This divergence is detectable in the dimension of covariation relating 'robusticity' and 'twist-flexing' between the humerus and the coracoid (Fig. 5B). This trend is possibly a consequence of differential bone growth rate, given that the relative perimeter of growth of the long bone shafts in amniotes bears a significant phylogenetic signal (Cubo *et al*., 2008). Furthermore, Deeming & Ferguson (1990) showed that size, from stage to stage in development, increased faster in *A. mississippiensis* than in *C. porosus* and *Crocodylus johnstoni*, and related this phenomenon to greater genetic growth control in *Alligator*. The robusticity of the appendicular elements studied is congruent with other aspects of alligatorid evolution, such as the presence of wide skulls and highly ossified structures (e.g. rostral canthi in *Melanosuchus*; palpebrals in *Paleosuchus*; double ossified scales in *Caiman*). This phenomenon should be extrapolated to the alligatorid lineage in further studies of embryonic development.

The macroevolutionary dimension

Our last level of organismic analysis concerns the phenotypic similarity among crocodylians in a macroevolutionary context. The fact that Alligatoridae, Crocodylidae, and *Tomistoma* + *Gavialis* share patterns of variation and integration of the anterior appendage suggests, by phylogenetic inference, that at least the most recent common ancestor of the crown group would have shared the same pattern (i.e. a high level of forelimb integration plus a coracoid–humerus pair) in the Late Cretaceous (Fig. 7). Accordingly, the integration and shape variation patterns should be considered as a synapomorphy of the group (i.e. both patterns are homologous). However, to reinforce this hypothesis, we would need to consider the presence of this pattern in other extinct and more basal clades. The integration of the humerus–coracoid pair may be considered as an evolutionary module, encompassing both functional and developmental components (Brandon, 2005; Eble, 2005), if the concerted variation of the elements across clades pro-

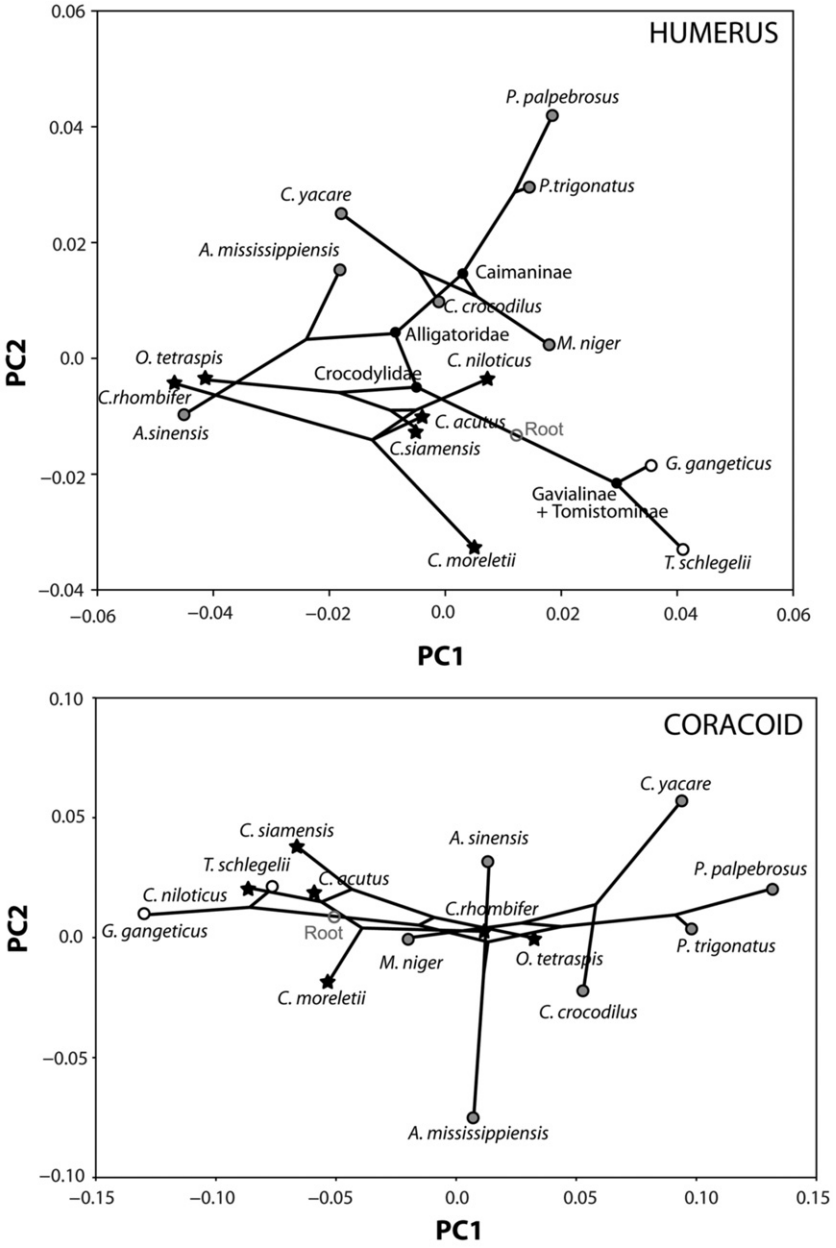

Figure 6. Phylogenetic tree of Figure 1 mapped on humerus and coracoid principal component analysis (PCA) (Figs 3C, 4A). Operational taxonomic units estimated using the minimum square change (branches are assumed to be equal length). The permutation tests confirm a phylogenetic signal of the data (humerus $P = 0.0039$; coracoid $P = 0.0006$ over 10 000 permutations). Root and nodes positions are depicted in humerus ordination. For the humerus, note the separation of Alligatoridae from the rest of crocodylians in the positive direction of PC2 and, for the coracoid, in the positive direction of PC1.

vides a basis for locomotion versatility in Crocodylia. Thus, the question arises of how the observed morphological integration of the coracoid–humerus pair was mediated by the acquisition of a modern semi-aquatic locomotion habit, if the evolutionary history of Crocodyliformes is delimited by differences between terrestrial (i.e. Notosuchia) and fully aquatic (Thalattosuchia, Dyrosauridae) or semi-aquatic life habits, which emerged within Neosuchia and includes the modern crocodylians (clade denomination according Jouve, 2009; Pol, Turner & Norell, 2009; Fig. 7A).

The available data on limb variation is limited, yet, so far, it suggest that the ratio and the scaling between elements (coracoid and humerus) is different

in the semi-aquatic forms (Fig. 7B; see also Supporting information, Appendix 2, comparing the allometric behaviour of measurements of extant species to that of extinct species of terrestrial and fully aquatic). In light of this, the morphology and proportion between the humerus and coracoid are: (1) notably different in basal Crocodyliformes (the terrestrial Cretaceous Gobiosuchidae) and (2) within mesoeucrocodylians, there are two phylogenetic steps: one that entails the relative enlargement of the coracoid and a second one that entails a relative reduction of the coracoid and the enlargement of the humerus that occurs within Crocodylia (see nodes 1 and 2 in Fig. 7A). Thus, the patterns of variation and integration appear to be phylogenetically shared by all crocodylian species, meaning that they stem from an inherited factor that was present, at least, in the most recent common ancestor of Crocodylia 65 Mya. The long-term stability of this evolutionary module could be a result of the joint action of selection and development, canalizing the morphological variance of the limb in Crocodylia. However, this should be verified by extrapolating the patterns to more ancient neosuchian taxa (e.g. the Late Jurassic family Goniopholididae), which are currently interpreted as semi-aquatic organisms (Buffetaut, 1982).

Within a phylogenetic framework, integration produces patterns of variation that help to address the way by which morphological evolution of the locomotor apparatus has taken place in crocodiles. The evolution of an integrated set of elements such as the humerus–coracoid pair, suggests that elements became functionally 'coupled' (Chernoff & Magwene, 1999) at the node Crocodylia. This coupling would denote an increase in the degree of integration between the bones that were previously not so strongly associated with the locomotion habits in terrestrial and fully aquatic mesoeucrocodylians. However, this issue would be best addressed quantitatively at hierarchically lower phylogenetic levels, by testing for differences in the pattern of integration of basal Crocodyliformes in comparison with Mesoeucrodylia.

Conclusions

The variation of single elements of the limb and girdle within Crocodylia indicates that the shape of each element changes significantly across species. Despite this, the disparity of these shape changes is constrained within two dimensions ('robusticity' and 'twist or flexing'). The suite of 3D shape variables capturing the geometry of each element is integrated, and there is a strong correlation between pairs of elements. In turn, we interpret that the unexpected integration between the coracoid and the humerus is a key innovation in Crocodylia in relation to a semi-aquatic life habit. Thus, the apparent phenotypic conservativeness in Crocodylia is underlined by a particular pattern of morphological integration (i.e. coupling). The analysis of the appendicular skeleton with geometric morphometrics (in 3D) opens a window for understanding the role of development and function in the evolution locomotor system in this group, and highlights the need to assess the function of the coracoid–humerus pair in further biodynamic and biomechanical studies.

ACKNOWLEDGEMENTS

We thank Dr Kenneth L. Krysko and Dr Max A. Nickerson (Florida Museum of Natural History, Gainesville, Florida). We are also grateful to Dr Santiago Reig Redondo and his research team (Laboratorio de Imagen Médica, Hospital General Universitario Gregorio Marañón, Madrid) for computed tomographic scanning of the bones used as the template.

Figure 7. A, pectoral girdle and forelimb morphologies in terrestrial (i.e. Notosuchia, *Simosuchus sensu* Sertich & Groenke, 2010), fully aquatic (Thalattosuchia, *Steneosaurus*; Andrews, 1913), and semi-aquatic life habits emerged in Crocodylia. The primitive configuration (left) corresponds to the terrestrial gobiosuchid from Las Hoyas (Ortega *et al*., 2000, based on the specimen MCCM-LH7991; Museo de las Ciencias de Castilla-La Mancha). Scale bar = 2.5 cm (0.5 cm for the gobiosuchid). The humerus is depicted in the dorsal view, the ulna in the medial view, and the radius in the dorsal view. Illustrations: *Simosuchus* is modified from Krause *et al*. (2010); *Steneosaurus* is modified from Anne Musser; *Paleosuchus* is modified from T. Pyrzakowsky (Ross & Magnusson, 1990); and the Las Hoyas gobiosuchid from Raul Martín originally drawn in 2003. The phylogenetic tree is scaled to geological time to give a sense of the evolution of the coracoid and humerus integration. Node 1 diagnoses the relative enlargement of the coracoid and relative humeral reduction, whereas Node 2 diagnoses the relative reduction of coracoids and the relative enlargement of the humerus. The dotted line below Node 2 indicates an uncertainty in estimating the age of emergence of coracoid–humerus integration in other semi-aquatic neosuchians. B, humeral (x-axis) and coracoid (y-axis) lengths are significantly linearly correlated in all of the three types of locomotions ($R^2 > 0.96$, $r > 0.98$ in all three cases, $P < 0.01$). However, the slopes are statistically different only in semi-aquatics relative to the other lifestyles ($P < 0.05$). The intercepts (analysis of covariance), on the other hand, are only different statistically between terrestrial and semi-aquatics ($P < 0.05$). This scaling difference is corroborated in the box and whisker plot of the ratio humerus/coracoids length, including outliers.

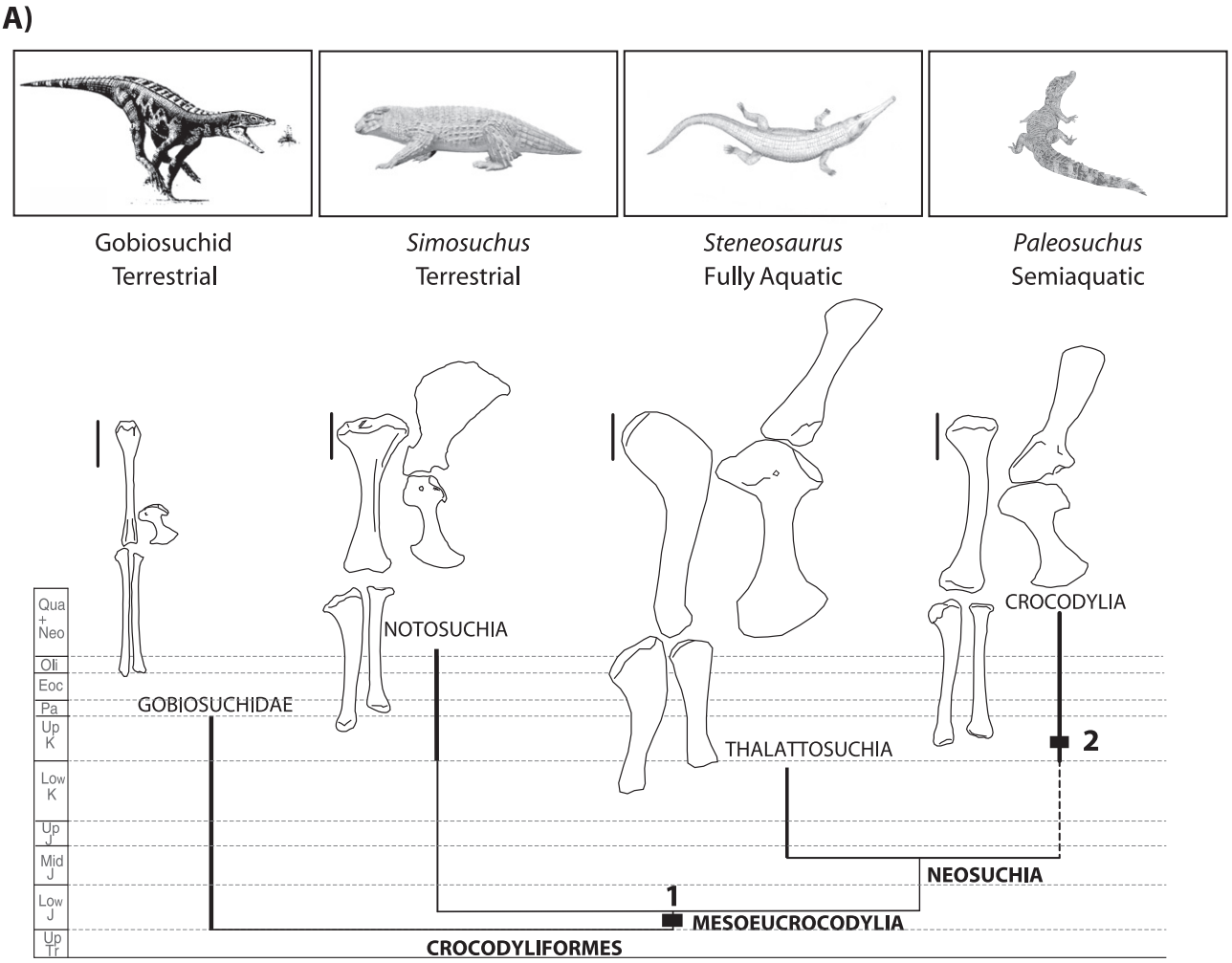
A)
Gobiosuchid
Terrestrial
Simosuchus
Terrestrial
Steneosaurus
Fully Aquatic
Paleosuchus
Semiaquatic
Qua + Neo
Oli
Eoc
Pa
Up K
Low K
Up J
Mid J
Low J
Up Tr
GOBIOSUCHIDAE
NOTOSUCHIA
THALATTOSUCHIA
CROCODYLIA
2
NEOSUCHIA
1
MESOEUCROCODYLIA
CROCODYLIFORMES

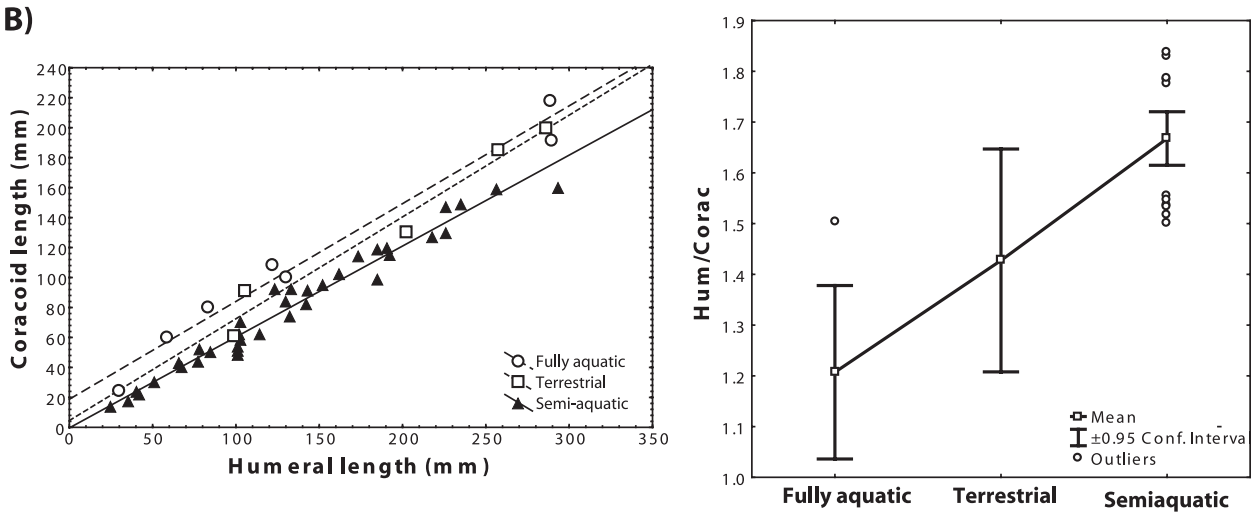
B)
Coracoid length (mm)
Humeral length (mm)
Fully aquatic
Terrestrial
Semi-aquatic
Hum/Corac
Mean
±0.95 Conf. Interva
Outliers
Fully aquatic
Terrestrial
Semiaquatic

The present work was supported by research project CGL2009-11838 BTE from the Spanish Government. B. Chamero was funded by an FPU grant from the MICINN (ref. AP2005-0677). We also thank the critical comments of Diego Pol, Eberhad Frey, and six anonymous referees, whose observations and questions notably contributed to improving this work.

REFERENCES

Andrews CW. 1913. *A descriptive catalogue of the marine reptiles from the Oxford Clay*. London: British Museum Natural History 2.

Arruda JT, Carvalho IS, Vasconcellos FM. 2004. Baurusuquídeos da Bacia Bauru (Cretáceo Superior, Brasil). *Anuário do Instituto de Geociências* **27:** 64–74.

Auffenberg W. 1954. Additional specimens of *Gavialosuchus americanus* (Sellards) from a new locality in Florida. *Quarterly Journal of the Florida Academy of Sciences* **17:** 185–209.

Benton MJ, Clark JM. 1988. Archosaur phylogeny and the relationships of the Crocodylia. In: Benton MJ, ed. *The phylogeny and classification of the tetrapods, volume 1: amphibians, reptiles, birds*. Systematics Association Special Volume No. 35A. Oxford: Clarendon Press, 295–338.

Bonnan MF, Sandrik JL, Nishiwaki T, Wilhite DR, Elsey RM, Vittore C. 2010. Calcified cartilage shape in archosaurs long bones reflects overlying joint shape in stress-bearing elements: implications for non-avian Dinosaur locomotion. *Anatomical Record* **293:** 2044–2055.

Bookstein FL. 1991. *Morphometric tools for landmark data: geometry and biology*. New York, NY: Cambridge University Press.

Brandon RN. 2005. Evolutionary modules: conceptual analyses and empirical hypotheses. In: Callebaut W, Rasskin-Gutman D, eds. *Modularity*. Cambridge, MA: MIT Press, 51–60.

Brochu CA. 1995. Heterochrony in the crocodylian scapulocoracoid. *Journal of Herpetology* **29:** 464–468.

Brochu CA. 1997a. Phylogenetic systematic and taxonomy of Crocodylia. DPhil Thesis, University of Texas, Austin.

Brochu CA. 1997b. Morphology, fossils, divergence timing, and the phylogenetic relationships of Gavialis. *Systematic Biology* **46:** 479–522.

Brochu CA. 1999. Phylogeny, systematic, and historical biogeography of Alligatoroidea. *Society of Vertebrate Paleontology Memoir* **6:** 9–100.

Brochu CA. 2011. Phylogenetic relationships of *Necrosuchus ionensis* Simpson, 1937 and the early history of caimanines. *Zoological Journal of the Linnean Society* **163:** 228–256.

Buffetaut E. 1982. Radiation évolutive, paléoécologie et biogéographie des Crocodiliens mésosuchienes. *Mémoires Societé Geologique de France* **142:** 1–88.

Buscalioni AD, Ortega F, Rasskin-Gutman D, Pérez-Moreno BP. 1997. Loss of carpal elements in crocodilian limb evolution: morphogenetic model corroborated by paleobiological data. Biological Journal of the Linnaean. *Society* **62:** 133–144.

Chernoff B, Magwene PM. 1999. Morphological integration: forty years later. In: Olson EC, Miller RL, eds. *Morphological integration*. London: The University of Chicago Press, 319–353.

Claessens LPAM. 2009. A cineradiographic study of lung ventilation in *Alligator mississippiensis*. *Journal of Experimental Zoology* **311A:** 563–585.

Cubo J, Legendre P, de Ricqlès A, Montes L, de Margerie E, Castanet J, Desdevises Y. 2008. Phylogenetic, functional, and structural components of variation in bone growth rate of amniotes. *Evolution and Development* **10:** 213–223.

Deeming DC, Ferguson MWJ. 1989. Effects of incubation temperature on the growth and development of embryos of *Alligator mississippiensis*. *Journal of Comparative Physiology* **159B:** 183–193.

Deeming DC, Ferguson MWJ. 1990. Morphometric analysis of embryonic development in *Alligator mississippiensis*, *Crocodylus johnstoni* and *Crocodylus porosus*. *Journal of Zoology* **221:** 419–439.

Desdevises Y. 2008. Phylogenetic, functional, and structural components of variation in bone growth rate of amniotes. *Evolution and Development* **10:** 213–223.

Dryden IL, Mardia KV. 1998. *Statistical shape analysis*. New York, NY: JW Wiley.

Eble GJ. 2005. Morphological modularity and macroevolution: conceptual and empirical aspects. In: Callebaut W, Rasskin-Gutman D, eds. *Modularity*. Cambridge, MA: MIT Press, 221–238.

Erickson GM, Gignac PM, Steppan SJ, Lappin AK, Vliet KA, Brueggen JD, Inouye BD, Kledzik D, Webb GJW. 2012. Insights into the ecology and evolutionary success of crocodilians reveals through bite-force and tooth-pressure experimentation. *PLoS ONE* **7:** 31781.

Farlow JO, Hurlburt GR, Elsey RM, Britton AR, Langston W. 2005. Femoral dimensions and body size of *Alligator mississippiensis*: estimating the size of extinct mesoeucroodylians. *Journal of Vertebrate Paleontology* **25:** 354–369.

Frey E. 1982. Ecology, locomotion and tail muscle anatomy of crocodiles. *Neues Jahrbuch Geologie Paläontologie Abhalungen* **164:** 194–199.

Frey E. 1988. Das Tragsystem der Krododile – eine biomechanische und phylogenetische Analyse. *Stuttgarter Beiträge zur Naturkunde, Serie A (Biologie)* **426:** 1–60.

Fujiwara S, Taru H, Suzuki D. 2010. Shape of articular surface of Crocodilian (Archosauria) elbow joints and its relevance to Sauropsids. *Journal of Morphology* **271:** 883–896.

Gatesy J, Amato G, Norell M, DeSalle R, Hayashi C. 2003. Combined support for wholesale taxic atavism in Gavialine Crocodylians. *Systematic Biology* **52:** 403–422.

Gatesy SM. 1991. Hind limb movements of the American alligator (*Alligator mississippiensis*) and postural grades. *Journal of Zoology* **224:** 577–588.

Gatesy SM, Middleton KM. 1997. Bipedalism, flight and the evolution of theropod locomotor diversity. *Journal of Vertebrate Paleontology* **17:** 308–329.

Jenkins FA. 1993. The evolution of the avian shoulder joint. *American Journal of Science* **293:** 253–267.

Jouve S. 2009. The skull of *Teleosaurus cadomensis* (Crocodylomorpha: Thalattosuchia), and phylogenetic analysis of Thalattosuchia. *Journal of Vertebrate Paleontology* **29:** 88–102.

Jouve S, Schwarz D. 2004. *Congosaurus bequaerti*, a Paleocene Dyrosaridae (Crocodyliformes; Mesoeucrocodylia) from Landana (Angola). *Bulletin de l'Institut Royal des Sciencies Naturelles de Belgique* **74:** 129–146.

Klingenberg CP. 2008. Morphological integration and developmental modularity. *Annual Review of Ecology, Evolution and Systematics* **39:** 115–132.

Klingenberg CP. 2009. Morphometric integration and modularity in configurations of landmarks: tools for evaluating a priori hypotheses. *Evolution & Development* **11:** 405–421.

Klingenberg CP. 2011. MorphoJ: an integrated software package for geometric morphometrics. *Molecular Ecology Resources* **11:** 353–357.

Klingenberg CP, Gidaszewski NA. 2010. Testing and quatifying phylogentic signal and homoplasy in morphometric data. *Systematic Biology* **59:** 245–261.

Krause DW, Sertich JJW, Rogers RR, Kast SC, Rasoamiaramanana AH, Buckley GA. 2010. Overview of the discovery, distribution and geological context of *Simosuchus clarki* (Crocodyliformes: Notosuchia) from the Late Cretaceous of Madagascar. *Journal of Vertebrate Paleontology* **30**(Suppl 6): 4–12.

Livingston VJ, Bonnan MF, Elsey RM, Sandrik JL, Wilhite DR. 2009. Differential limb scaling in the American alligator (*Alligator mississippiensis*) and its implications for archosaur locomotor evolution. *Anatomical Record* **292:** 787–797.

Maddison WP. 1991. Squared-change parsimony reconstructions of ancestral states for continuous-valued characters on a phylogenetic tree. *Systematic Zoology* **40:** 304–314.

Magwene PM. 2001. New tools for studying integration and modularity. *Evolution* **55:** 1734–1745.

Marugán-Lobón J, Buscalioni AD. 2006. Avian skull morphological evolution: exploring exo- and endocranial covariation with two-block partial least squares. *Zoology* **109:** 217–230.

Matsuoka T, Ahlberg PE, Kessaris N. 2005. Neural cresta origins of the neck and shoulder. *Nature* **436:** 347–355.

Meers MB. 2003. Crocodylian forelimb musculature and its relevance to Archosauria. *Anatomical Record (Part A)* **274A:** 891–916.

Mook CC. 1921. Notes on the postcranial skeleton in the Crocodilia. *Bulletin of the American Museum of Natural History* **44:** 67–100.

Müller GB, Alberch P. 1990. Ontogeny of the limb skeleton in *Alligator mississippiensis*: developmental invariance and change in the evolution of archosaur limbs. *Journal of Morphology* **203:** 151–164.

Nascimento PM, Zaher H. 2010. A new species of Baurusuchus (Crocodyliformes, Mesoeucrocodylia) from the Upper Cretaceous of Brazil, with the first complete postcranial skeleton described for the family Baurusuchidae. *Papéis Avulsos de Zoologia* **50:** 323–361.

Olson EC, Miller RL. 1958. *Morphological integration*. London: University of Chicago Press.

Ortega F, Gasparini Z, Buscalioni AD, Calvo JO. 2000. A new species of Araripesuchus (Crocodylomorpha) from the Lower Cretaceous of Patagonia. *Journal of Vertebrate Paleontology* **20:** 57–76.

Osmólska H, Hua S, Buffetaut E. 1997. Gobiosuchus Kielanae (Protosuchia) from the Late Cretaceous of Mongolia: anatomy and relationships. *Acta Palaeontologica Polonica* **42:** 257–289.

Piras P, Teresi L, Buscalioni AD, Cubo J. 2009. The shadow of forgotten ancestors differently constraints the fate of Alligatoroidea and Crocodyloidea. *Global Ecology and Biogeography* **18:** 30–40.

Pol D. 2005. Postcranial remains of *Notosuchus terrestris* Woodward (Archosauria: Crocodyliformes) from the upper Cretaceous of Patagonia, Argentina. *Ameghiniana (on line)* **42:** 21–38.

Pol D, Turner AH, Norell MA. 2009. Morphology of the Late Cretaceous Crocodylomorph *Shamosuchus djadochtaensis* and a discussion of Neosuchian phylogeny as related to the origin of Eusuchia. *Bulletin of the American Museum of Natural History* **324:** 1–103.

Rasskin-Gutman D, Buscalioni AD. 2001. Theoretical morphology of the archosaur (Reptilia: Diapsida) pelvic girdle. *Paleobiology* **28:** 59–78.

Reilly SM, Elias JA. 1998. Locomotion in *Alligator mississippiensis*: kinematic effects of speed and posture and their relevance to the sprawling-to-erect paradigm. *Journal of Experimental Biology* **201:** 2559–2574.

Reilly SM, Willey JS, Biknevicius AR, Blob RW. 2005. Hindlimb function in the alligator: integrating movements, motor patterns, ground reaction forces and bone strain of terrestrial locomotion. *Journal of Experimental Biology* **208:** 993–1009.

Riff D, Kellner WA. 2011. Baurusuchid crocodyliforms as theropod mimics: clues from the skull and appendicular morphology of *Stratiotosuchus maxhechti* (Upper Cretaceous of Brazil). *Zoological Journal of the Linnean Society* **163:** 37–56.

Riska B. 1986. Some models for development, growth, and morphometric correlation. *Evolution* **40:** 1303–1311.

Rohlf FJ. 2002. Geometric morphometrics and phylogeny. In: MacLeod N, Forey PL, eds. *Morphology, shape, and phylogeny*. London: Taylor & Francis, 175–193.

Rohlf FJ, Corti M. 2000. Use of two-block partial least-squares to study covariation in shape. *Systematic Biology* **49:** 740–753.

Rohlf FJ, Slice DE. 1990. Extensions of the Procrustes method for the optimal superimposition of landmarks. *Systematic Zoology* **39:** 40–59.

Romer AS. 1924. Pectoral limb musculature and shoulder-girdle structure in fish and tetrapods. *Anatomical Record* **27:** 119–143.

Ross CA, Magnusson WE. 1990. Les crocodiliens actuels. In:

Ross CA, Garnett S, eds. *Crocodiles, alligators et caimans*. Bordas: Encyclopedie Visual, 58–73.

Sadleir RW, Makovicky PJ. 2008. Cranial shape and correlated characters in crocodilian evolution. *Journal of Evolutionary Biology* **21:** 1578–1596.

Salisbury SW, Frey E. 2001. A biomechanical transformation model for the evolution of semi-spheroidal articulations between adjoining vertebral bodies in crocodilians. In: Grigg CG, Seebacher F, Franklin CE, eds. *Crocodylian biology and evolution*. Chipping Norton: Surrey Beatty & Sons, 85–134.

Salisbury SW, Molnar RE, Frey E, Willis PMA. 2006. The origin of modern crocodyliforms: new evidence from the Cretaceous of Australia. *Proceedings of the Royal Society of London Series B, Biological Sciences* **273:** 2439–2448.

Schwarz D, Frey E, Martin T. 2006. The postcranial skeleton of the Hyposaurinae (Dyrosauridae, Crocodyliformes). *Palaeontology* **49:** 695–718.

Sertich JJ, Groenke JR. 2010. Appendicular skeleton of *Simosuchus clarki* (Crocodyliformes, Notosuchia) from the late Cretaceous of Madagascar. *Journal of Vertebrate Paleontology* **30** (Suppl 6)**:** 122–153.

Shubin N, Tabin C, Carroll S. 1997. Fossils, genes and the evolution of animal limbs. *Nature* **388:** 639–648.

Suzuki D, Murakami G, Minoura N. 2003. Crocodilian bone–tendon and bone–ligament interfaces. *Annals of Anatomy* **185:** 425–433.

Villmoare B, Fish J, Jungers W. 2011. Selection, morphological integration and strepsirrhine locomotor adaptations. *Evolutionary Biology* **38:** 88–99.

Wermuth H, Fuchs K. 1978. *Bestimmen von Krokodilenm und ihrer Häute*. Stuttgart: Gustav Fischer Verlag.

Wiley DF. 2006. *Landmark Editor*, Version 3.0. Available at: http://graphics.idav.ucdavis.edu/research/EvoMorph

Willey JS, Biknevicius AR, Reilly SM, Earls KD. 2004. The tale of the tail: limb function and locomotor mechanics in *Alligator mississippiensis*. *Journal of Experimental Biology* **207:** 553–563.

Wu X-C, Russel AP, Cumbaa SL. 2001. Terminonaris (Archosauria: Crocodyliformes): new material from Saskatchewan, Canada, and comments on its phylogenetic relationships. *Journal of Vertebrate Paleontology* **21:** 492–514.

Young NM. 2006. Function, ontogeny and canalization of shape variance in the primate scapula. *Journal of Anatomy* **209:** 623–636.

Young NM, Hallgrímsson B. 2005. Serial homology and the evolution of mammalian limb covariation structure. *Evolution* **59:** 2691–2704.

SUPPORTING INFORMATION

Additional Supporting Information may be found in the online version of this article:

Appendix S1. List of the specimens examined from the collection of the Florida Museum of Natural History (UF). The absence (O) or presence (X) of elements is indicated for each specimen. Information on age and sex were not available for all the specimens; instead, femoral length in mm (FL) is provided as a reference of body size.

Appendix S2. Metric data (lengths in mm) used contrasting the distinct humeral and coracoid scaling and ratios relative to locomotion and ambient (Fig. 7). Crocodylia represents a semi-aquatic condition in comparison with fully terrestrial and aquatic mesoeucrocodylians. Gobiosuchidae is taken as the sister group of Mesoeucrocodylia. CAT, locomotion category (Aq, fully aquatic; SmA, semi-aquatic; T, terrestrial); CL, coracoid length; HL, humeral length, H/C, humeral/coracoid ratio; SIGNAT, specimen signature.